Video Matching

Peter Sand and Seth Teller*
MIT Computer Science and Artificial Intelligence Laboratory

November 11, 2004

Abstract

This paper describes a method for bringing two videos (recorded at different times) into spatiotemporal alignment, then comparing and combining corresponding pixels for applications such as background subtraction, compositing, and increasing dynamic range. We align a pair of videos by searching for frames that best match according to a robust image registration process. This process uses locally weighted regression to interpolate and extrapolate high-likelihood image correspondences, allowing new correspondences to be discovered and refined. Image regions that cannot be matched are detected and ignored, providing robustness to changes in scene content and lighting, which allows a variety of new applications.

1 Introduction

Given multiple still images of a scene from the same camera center, one can perform a variety of image analysis and synthesis tasks, such as foreground/background segmentation, copying an object or person from one image to another, building mosaics of the scene, and constructing high dynamic range composites.

Our goal is to extend these techniques to video footage acquired with a moving camera. Given two video sequences (recorded at separate times), we seek to spatially and temporally align the frames such that subsequent image processing can be performed on the aligned images. We assume that the input videos follow nearly identical trajectories through space, but we allow them to have different timing. The output of our algorithm is a new sequence in which each "frame" consists of a pair of registered images. The algorithm provides an alternative to the expensive and cumbersome robotic motion control systems that would normally be used to ensure registration of multiple video sequences. (In these systems, a camera is attached to a robotic arm/platform that can be program to repeat the same camera move multiple times.)

The primary difficulty in this task is matching images that have substantially different appearances (Figure 1). Video sequences of the same scene may differ from one another due to moving people, changes in lighting, and/or different exposure settings.

*e-mail: {sand,teller}@csail.mit.edu

In order to obtain good alignment, our algorithm must make use of as much image information as possible, without being misled by image regions that match poorly.

Traditional methods for aligning images include feature matching and optical flow. Feature matching algorithms find a pairing of feature points from one image to another, but they do not give a dense pixel correspondence. Optical flow produces a dense pixel correspondence, but is not robust to objects present in one image but not the other.

Our method combines elements of feature matching and optical flow. In a given image, the algorithm identifies a set of textured image patches to be matched with patches in the other image. Once a set of initial matches has been found, we use these matches as motion evidence for a regression model that estimates dense pixel correspondences across the entire image. These estimates allow further matches to be discovered and refined using local optical flow. Throughout the process, we estimate and utilize probabilistic weights for each correspondence, allowing the algorithm to detect and discard (or fix) mismatches.

Our primary contribution is a method for spatially and temporally aligning videos using image comparisons. Our image comparison method is also novel, insofar as it is explicitly designed to handle large-scale differences between the images. The main limitation of our approach is that we require the input videos to follow spatially similar camera trajectories. The algorithm cannot align images from substantially different viewpoints, partially because it does not model occlusion boundaries. Nonetheless, we demonstrate a variety of applications for which our method is useful.

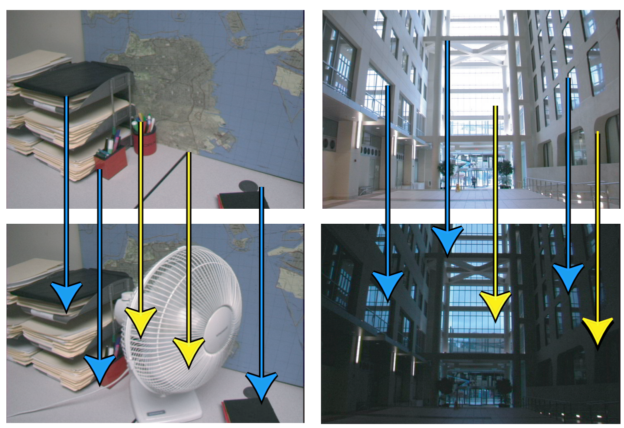

Figure 1: Our matching algorithm is robust to differences such as an object that appears in only one image (left pair) or changes in lighting and exposure (right pair). The key idea behind our matching algorithm is to identify which parts of the image can be matched (blue arrows) without being confused by parts of the image that are difficult or impossible to match (yellow arrows).

2 Related Work

Aligning a pair of images is a standard problem in computer vision. Optical flow algorithms [1] find a vector field that maps each pixel from one image to a corresponding pixel in another image. Stereo methods [2] use known camera poses to restrict the search to 1D lines (for images of a static scene). Many of these algorithms are robust to small-scale effects (such as local violations of smoothness or reflectance assumptions), but they are not intended for matching images that have large differences in lighting or have large objects that appear in one image but not the other. Some flow estimation methods [3] handle large image regions that do not match by robustly fitting global parametric models to local flow estimates. Our method fits a non-parametric model and does not rely entirely on local flow estimates.

The basis of our algorithm is matching salient image points [4, 5]. Many existing methods prune feature matches using robust fitting methods (such as RANSAC [6]) with constraints from the fundamental matrix [7]. Brown and Lowe [5] align images by matching features that are invariant to several spatial and illumination transformations. Kanazawa and Kanatani [8] find good correspondences using epipolar constraints combined with smoothness and spatial consistency criteria. Smith *et al.* [9] refine feature matches by comparing the length and angle of each correspondence vector with its neighbors.

None of these image correspondence techniques addresses the larger problem of video registration. Caspi and Irani [10] align video sequences using a single image transformation and single time offset for an entire sequence. This method is successful for rigidly connected cameras that simultaneously record a scene, but does not apply to spatially or temporally different motions. Sawhney *et al.* [11] provide a method of aligning two video sequences using stereo and optical flow, but also aim only at the case of rigidly connected cameras simultaneously recording a scene. Rao *et al.* [12] temporally match video sequences by tracking a feature that appears in each video and aligning the resulting trajectories. This requires a user-specified trackable feature and does not provide dense pixel correspondences between the video sequences.

Our method provides a warping field and temporal offset for each frame, allowing the video frames to be registered for various segmentation and compositing applications. Several of these applications have been addressed via different methods. Chuang *et al.* [13] use mosaicing techniques to reconstruct a background image that is used for foreground segmentation. Kang *et al.* [14] register images at different exposures to obtain high dynamic range video. These applications and others can be performed with the help of the method we present in this paper.

3 Overview

Our goal is to construct a mapping between two videos so that both videos can be manipulated in a shared spatial and temporal domain. One of the two videos is designated as the primary video, the other as the secondary. The primary video provides the spatial and temporal reference; the secondary video is mapped to match it.

The core of the algorithm is robust image alignment, described in Section 4, which provides a warping from one image to another that is robust to significant differences between those images. This image alignment technique is used as a sub-function of the video alignment process, which is described in Section 5. In Section 6, we present two extensions to the basic algorithm. We describe experimental evaluations in Section 7 and give various applications in Section 8. Limitations and planned solutions to these limitations are discussed in Section 9.

4 Robust Image Alignment

Our image alignment algorithm finds correspondences between pixels in a pair of images. Each correspondence is assigned a weight according to the likelihood that it describes a physical 3D point undergoing a physical 3D motion. The ability to characterize the correctness of a correspondence is essential to the robustness of the algorithm. We want to use as much information from the images as possible, but we do not want to be misled by unexpected differences between the images.

The weight w_i assigned to the i^{th}correspondence is the product of two terms: a pixel matching probability P_i (Section 4.2) and a motion consistency probability M_i (Section 4.3). For simplicity, we assume independence when combining the probabilities.

4.1 Local Contrast and Brightness Normalization

To handle cases with a substantial change in lighting or exposure between the primary and secondary videos, we pre-process the videos to remove differences in brightness and contrast. To simplify the normalization process, we begin by converting each frame to a grayscale image $I(x,y)$.

For a given pixel (x,y), we compute the brightness and contrast for a region R centered around the pixel (we use 24-by-24-pixel squares). The brightness is characterized by the mean pixel value over R, denoted as $I_{mean}(x,y)$. The contrast is computed from the difference between the minimum and maximum values over R, denoted as $I_{min}(x,y)$ and $I_{max}(x,y)$. To maintain stability in regions with low contrast, the algorithm bounds the contrast from below. We compute the contrast $C(x,y)$ using a parameter c_{thresh} that we set to 30:

$$C(x,y) = max(I_{max}(x,y) - I_{min}(x,y), c_{thresh}) \tag{1}$$

To compute the normalized pixel, we use the following equation, which subtracts the brightness and divides by the contrast:

$$I_{norm}(x,y) = 0.5 + \frac{I(x,y) - I_{mean}(x,y)}{C(x,y)} \tag{2}$$

Here we assume pixel intensities can range from 0 to 1. Pixel values that fall outside the 0 to 1 range after the process are clipped to lie within the range.

The resulting normalized image is partially invariant to local changes in illumination. This invariance is sufficient to allow subsequent comparison of pixel values between images that were originally recorded at different exposures or under different lighting conditions.

4.2 Pixel Consistency

To compute the pixel matching probability, P_i, for a particular correspondence, we evaluate how well the images match in a square region around the correspondence. Rather than simply comparing pixel values, we use a method that allows small spatial variations in the corresponding pixel locations. This technique, inspired by Birchfield and Tomasi [15], permits small changes in scale, rotation, and skew of an image region due to differences in camera viewpoint. This also alleviates several sampling issues. (Similar methods are proposed by Kutulakos [16] and Szeliski and Scharstein [17].)

A single pixel in the primary image is compared with a 3-by-3 neighborhood of pixels in the secondary image, rather than with a single secondary pixel. To do this efficiently, the algorithm applies 3-by-3 minimum and maximum filters to the secondary image, producing new images I_{min} and I_{max} (Figure 2). (Note that these min and max images are not the same as the min and max images in the previous section.) These minimum and maximum images define bounds on the value of each pixel in the secondary image; the corresponding primary pixel receives a penalty if and only if its value lies outside this interval.

To evaluate a correspondence, our algorithm sums this pixel matching score across a square region (with size specified in Section 7). For an image region R in the primary image I we obtain the following score:

$$\sum_{(x,y)\in R} max(0, I(x,y) - I_{max}(x+u, y+v), I_{min}(x+u, y+v) - I(x,y)). \tag{3}$$

Here u and v describe an offset from a point (x,y) in the primary image to the corresponding point $(x+u, y+v)$ in the secondary image (the same offset is used across the entire region). We average the above score over each color channel to obtain the pixel intensity dissimilarity d_i for the i^{th}correspondence.

In the case that the primary and secondary images contain substantial differences in lighting or exposure, we perform local brightness and contrast normalization, as described in Section 4.1. This normalization can be thought of as a pre-processing step; once the images are normalized, the rest of algorithm remains the same as the un-normalized case.

In either case, we use the pixel intensity dissimilarity d_i to compute the pixel matching probability P_i:

$$P_i = N(d_i, \sigma^2_{pixel}). \tag{4}$$

Here $N(x, \sigma^2)$ is a zero-mean Gaussian with variance σ^2 evaluated at x. We specify σ_{pixel} as described in Section 7.

This method of comparing image regions attains some invariance to affine transformations, but not as much as other methods [5, 18]. In our case, the region can be distorted by about a pixel and still successfully match (with zero penalty), while further distortion is penalized. Stronger distortion invariance is not necessary for our algorithm, because we limit the input images to have similar viewpoints.

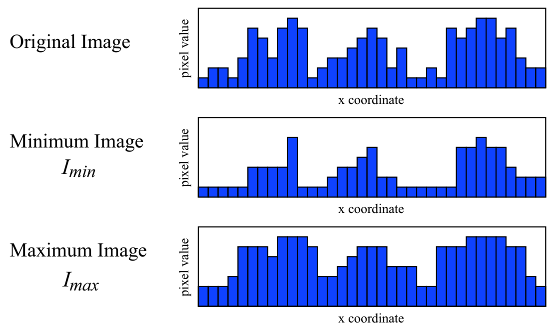

Figure 2: Each plot represents a cross section of a hypothetical image. The image is (non-linearly) filtered so each pixel becomes the minimum or maximum of its 3 by 3 neighborhood.

4.3 Motion Regression and Consistency

To evaluate motion consistency, we determine how well the offset vector (u,v) of a particular correspondence agrees with its neighbors. This requires initial estimates of the weights $\{w_i\}$ for the other correspondences, which we will obtain as described in Section 4.4. From these weights and the correspondences $\{(x_i,y_i,u_i,v_i)\}$, the algorithm reconstructs a vector field $u(x,y)$, $v(x,y)$ that provides an offset for each pixel of the primary image.

Our algorithm computes $u(x,y)$ and $v(x,y)$ using locally weighted linear regression [19], which determines the value of a function at a query point by fitting a regression model to nearby points, each weighted by its distance to the query point. The smoothness of locally weighted regression is determined by a kernel width parameter, K, describing the shape of the distance weighting function (typically a Gaussian). We modify this method to incorporate our correspondence probabilities by multiplying the kernel weight for each correspondence by its matching weight w_i.

We make one additional modification to standard locally weighted regression: we adapt the kernel width according to the density of points around the query point (Figure 3). We increase the kernel width K in regions of low data density (to bridge large gaps) and decrease K in regions of high data density (to model fine details). To do this, the algorithm sets K to the average distance from the query point to the N nearest neighbors. (N is one of the parameter values given in Section 7.) This adaptive kernel width is particularly useful for image correspondences, which may occur densely in highly texture regions, but very sparsely elsewhere (such as untextured walls and floors).

A linear model for u and v in terms of x and y can describe image-space rotation, scaling, and other affine transformations. By using locally weighted regression, we extend the linear model to describe smooth image warps, including lens distortion and gradual variations due to depth and perspective. One advantage of fitting a local model is that we expect to extrapolate better than simply averaging nearby points (Figure 3). (Note in the figure that the averaging levels off outside the data, whereas regression-based methods continue to extrapolate upward or downward outside the data.)

In order to compute the motion consistency probability M_i for a correspondence, the algorithm compares the previously assigned vector (u_i, v_i) with the vector $(\hat{u}_i, \hat{v}_i)$ predicted by adaptive locally weighted regression. The motion consistency probability is based on the difference between these two vectors:

$$M_i = N(\sqrt{(u_i - \hat{u}_i)^2 + (v_i - \hat{v}_i)^2}, \sigma^2_{motion}). \quad (5)$$

We experimented with a fundamental matrix model but found that it was redundant with the motion regression; in our test sets, the correspondences that satisfy the fundamental matrix also have high motion consistency probability.

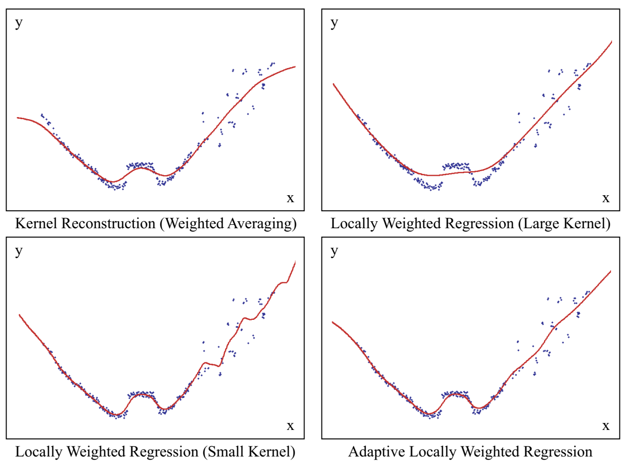

Figure 3: Each plot represents a generic regression problem in which we seek to fit a function $y(x)$. Weighted averaging does not extrapolate the function beyond the given data. Locally weighted linear regression does extrapolate, but leaves an issue of selecting the best kernel size. When the data density is highly variable, we prefer to adjust the kernel size according to the local density. We use adaptive locally weighted regression to interpolate and extrapolate correspondences, resulting in a dense correspondence field.

4.4 Finding Good Correspondences

Now that we have a way of evaluating the quality of a correspondence, we can attempt to find a number of good correspondences between a pair of images. To compute the motion consistency probabilities, we must bootstrap the algorithm with some good initial guesses.

The algorithm begins by selecting feature points using a Harris corner detector [4] (with a modification from page 45 of Noble's thesis [20]). Each feature point in the primary image is compared with the feature points in the secondary image to find good matches according to nearby pixel values. These initial matches are used to find preliminary regression predictions. (Each initial match is assigned a weight according to the pixel matching probability, then those weights are used to compute regression predictions, which are in turn used to modify the weights.)

For each feature point in the primary image, we then search for the most likely match in the secondary image according to the correspondence weighting function (including both pixel matching and motion consistency). The algorithm checks for matches in the secondary image at the location predicted by the regression function and at various nearby feature points found by the corner detector. For each candidate location, the algorithm performs a local motion optimization using the KLT method [21, 22]. Because the KLT optimizer is initialized with regression predictions, it can find good correspondences even when the feature detector fails to find the same points in each image. The local motion optimization allows sub-pixel correspondences, which we would not obtain simply by matching feature-detector maxima.

After trying to improve each correspondence, the algorithm recomputes the regression predictions and repeats the pointwise correspondence optimization (in a manner similar to EM [23]). Termination occurs when an iteration completes without making further improvement.

An advantage of this EM-like method over an alternative such as RANSAC [6] is that our algorithm can alter the correspondences (through the use of regression and local motion optimization) to obtain better correspondences after an initial pairing. In an image matching context (as opposed to 3D reconstruction), Kanazawa and Kanatani [8] demonstrate that an iterative feedback algorithm performs better than RANSAC.

After finding a set of high likelihood correspondences, we use the locally weighted regression method described in Section 4.3 to interpolate and extrapolate the offset vectors, obtaining a dense correspondence field.

5 Video Matching

The robust image alignment method described in the previous section is the primary component of our video matching algorithm. Given the image alignment method, the video matching process is relatively simple. We search for possible pairings between frames in the primary and secondary videos using the image alignment algorithm to evaluate candidate frame matches.

For each primary frame, once a matching secondary frame has been found, the secondary frame is warped into alignment with the primary frame. The output of the algorithm is a new version of the secondary video that is spatially and temporally registered with the primary video.

5.1 Frame Matching Measure

To evaluate the quality of a match between a pair of frames, we use the robust image alignment method (Section 4) to find a correspondences between the frames, then use the correspondences to estimate how well the primary and secondary frames match. Below we describe several methods for characterizing the quality of a frame match.

5.1.1 Correspondence Magnitude

The simplest measure is the magnitude of the correspondence vectors. We seek to minimize this value:

$$\sum_i w_i(u_i^2 + v_i^2) \tag{6}$$

This measure encourages overlap between the frames. Sometimes the horizontal overlap is more important than the vertical overlap (or vice versa), in which case the u_i and v_i components can be weighted appropriately.

5.1.2 Approximate Parallax

Another measure of the quality of the match between a pair of frames is the amount of parallax in the mapping between the images. Our parallax measure quantifies the amount of depth-induced relative motion between the correspondences. We minimize parallax because depth discontinuities will cause errors in the reconstructed correspondence field.

Let (x_i, y_i, x_i', y_i') denote a correspondence between two images. Here (x_i, y_i) is a position in one image and (x_i', y_i') is the corresponding position in the other image (or in the earlier notation: $x_i' = x_i + u_i$ and $y_i' = y_i + v_i$).

For two correspondences, indexed by i and j, the algorithm computes the distance between the pair of points in the primary image:

$$\delta_{ij} = \sqrt{(x_i - x_j)^2 + (y_i - y_j)^2} \tag{7}$$

and similarly the distance between the corresponding points in the secondary image:

$$\delta_{ij}' = \sqrt{(x_i' - x_j')^2 + (y_i' - y_j')^2} \tag{8}$$

A difference between these distances indicates parallax. So we take the weighted average of differences between these distances:

$$\sum_{ij} w_i w_j (\delta_{ij} - \delta_{ij}')^2 \tag{9}$$

This sum is indexed over all pairs of correspondences. Because the correspondences are relatively sparse, this value can be computed quite quickly.

The parallax measure is invariant to image-plane rotation and translation, but not invariant to looming motions and depth effects (the quantities we wish to detect). The parallax measure is most appropriate for translational camera motions, in which the correspondence magnitude measure will not generally provide the best match. However, for rotational camera motions, the parallax measure is not useful, because it should always be near zero.

5.1.3 Image Difference

Another characterization of the quality of a frame match is the difference between the primary frame and the projected secondary frame. This would seem to be the natural characterization of the quality of a frame match (it measures how well the match succeeded in aligning the pixels), but it has some drawbacks. One problem is that the measure is sensitive to the differences (in content or lighting) between the images. More significant, this criterion is hard to optimize, because it does not have a well behaved shape as an objective function. Nonetheless, it may be useful for choosing the best frame match in combination with the others.

5.1.4 A Combination

Often the best frame matching measure is a combination of the measures described above. We found that a sum of the parallax measure and correspondence magnitude (with a higher weighting on parallax) worked well for our demos (which include both rotational and translational camera motion). However, different combinations may be necessary for some sequences.

5.2 Adaptive Search for Matching Frames

Using the objective function described in Section 5.1, we wish to search the secondary video for a good match to a particular frame in the primary video. For computational efficiency, we do not want to evaluate the objective function for every frame of the secondary video, but instead select a small subset of frames to consider.

Given some initial guess of where to look in the secondary video, our algorithm evaluates several nearby frames and fits a quadratic regression model to the objective function values of these pairings (Figure 5). These preliminary evaluations occur at the initial guess, 1 frame forward, 1 frame backward, 5 frames forward, and 5 frames backward. The algorithm then checks frames near the minimum of the quadratic model and re-estimates the model after each new observation of the objective function. Once all secondary frames near the quadratic minimum have been checked, the algorithm picks the one with the lowest objective function value.

In order to compute an initial guess for the next frame search, the algorithm computes a weighted average of the changes between the frame indices of the prior matches. The weights decay by $1/2$ for each frame and are truncated after 5 frames. This weighted average is added to the previous frame index to obtain a starting point for the search for the next frame. The decaying weights allow the algorithm to respond to changes in the relative camera velocity between the videos, but with some damping to avoid over-reacting to these changes.

For the first frame of the primary video, we have no previous evidence for where to look in the secondary video. We do not need to know the particular frame that will match best, but we need a good enough guess to initiate the quadratic search. This initial guess can be provided by the user or found automatically by a linear search of the secondary video.

This search method allows substantial flexibility in the temporal mapping from one video to the other. One video can be much faster than the other or proceed in the opposite direction. The videos can change speed and relative direction, so long as the changes are smooth. A video graph (Section 6) can be used to handle discontinuous temporal mappings.

6 Optional Variations

6.1 Fast Frame Matching

In order to speed up the video matching process, we quickly estimate the quality of the match between a pair of frames. To do this, we run the image matching algorithm (Section 4.4), but skip the KLT motion optimization (the part of the process that takes the most time). This results in less accurate correspondences, but does not substantially affect the correspondence properties that are used to select matching frames as described in Section 5.1. Once we have found a good frame match, we re-run the full algorithm to obtain accurate pixel correspondences.

6.2 Video Graph Matching

For some applications, the secondary video may include many passes over a single background environment. In this case, rather than searching for frame matches within a temporal window of the second video, we would like to consider possible matches scattered throughout the video.

To do this, we build a video graph, in which each frame is a node and edges are created between frames that have a similar pose, as determined by the image alignment algorithm. A video graph is like a video texture [24], but designed to handle variations in camera pose. We have experimented with various ways to build a video graph quickly, such as using histograms and low-res optical flow to compare images quickly before decided to perform more expensive comparisons. Of course, building a video graph raises the question of how to set the threshold for creating an edge between two frames. We typically set this threshold such that a pair of frames are connected if our method can warp between the frames without significant artifacts.

To perform video matching, the algorithm searches the graph for good matches, starting at the best match found for the previous frame. In this case, we replace the quadratic frame search described in Section 5.2 with a more simplistic search. We evaluate the previous frame match and each frame connected to it. We then select the best match and evaluate the frames connected to it. This process repeats until all frames connected to the best frame have been evaluated. The best frame is designated as the match for the current primary frame and used to start the search for the next primary frame.

Video graphs allow the frame search process to consider a range of nearby viewpoints, regardless of their original temporal ordering. This allows a single primary frame to be matched to a frame from one of several different secondary videos. Video graphs can also be useful when the frame mapping is discontinuous (such as when one video makes an excursion off the path of the other, then returns to continue matching the other path).

7 Experimental Evaluation

To characterize the quality of a video match, we warp each secondary frame into the corresponding primary frame and compare pixel values. To avoid sampling artifacts, we use the min/max pixel comparison method described in Section 4.2. We take the mean over the pixels in each frame (not including the pixels for which the primary and secondary frames do not overlap), averaged over all the frames in the primary video sequence.

This produces a single number that represents the quality of the video match. Using this measure, we can explore various design changes (such as verifying that fundamental matrix constraints do not improve the results). We can also set the algorithm's parameters by determining which values give the best scores on a training set.

For our experiments, we set the algorithm's parameters using a training set consisting of a variety of different sequences (with different kinds of motion and different kinds of scenes). Because there is little danger of overfitting, we expect these same parameters to perform well on other sequences. For the feature detector (Section 4.4), we use a Gaussian window with a standard deviation of 5 pixels and a detector threshold of 1.0. The feature detector enforces a minimum spacing of 12 pixels between feature points. The algorithm computes the pixel dissimilarity for a correspondence using a 24 by 24 pixel region. The search for initial matches is restricted to be within 100 pixels of each primary frame feature point. We use the average distance to the nearest 80 points to set the adaptive kernel width for locally weighted regression. We set $\sigma_{pixel} = 2$ and $\sigma_{motion} = 10$.

On a set of 200 image pairs from four different kinds of scenes, the algorithm had an average running time of 1.31 seconds for each image pair (on a single-processor desktop PC). The majority of this time is spent on the KLT optimization described in Section 4.4. Performing the complete video matching algorithm (with multiple image comparisons per frame) takes several minutes per second of primary video. The fast matching method described in Section 6 improves the overall running time by about a factor of seven.

8 Applications

The ability to register video sequences has a variety of applications. As illustrated by Agarwala *et al.* [25], a set of registered images provides numerous opportunities for image manipulation. The video matching algorithm described in this paper allows these operations to be performed on frame sequences from moving cameras. We demonstrate several of these applications in the video available on the 2004 SIGGRAPH DVD.

The output of the video matching algorithm is a new version of the secondary video in which each frame is registered with the corresponding frame of the primary video. Given this aligned secondary video, pixels can be copied over, compared with, and blended with pixels from the primary video using standard commercial compositing software.

8.1 Background Subtraction

Given an image containing objects and an empty background image without the objects, the objects can be localized by comparing corresponding pixels (Figure 4). Tracking a moving object enables tasks such as gesture recognition, surveillance, and markerless motion capture [26]. If the object is visually different from the background, accurate object boundaries can be found, providing mattes for various of filmmaking applications. These mattes can be improved using more sophisticated methods [13].

8.2 Compositing

Aligning two video sequences allows pixels to be copied from one to the other (Figure 9). An empty street with an action sequence can be composited onto a street full of traffic. A blue sky can be composited onto a shot that had a gray sky. People and objects can be added to or repeated in a scene. In many cases, a rough matte is sufficient for this kind of compositing, because the background is assumed to be the same in both sequences. If a precise matte is needed, it can be obtained by background subtraction, color segmentation, or semi-automatic rotoscoping.

In our video, we demonstrate several kinds of compositing. To make the mugs and glasses disappear and reappear, we simply fade between a sequence that contains the objects and another sequence that does not contain the objects. To make the tree grow and shrink, we transition between the primary and secondary sequence using a procedurally generated matte. The disembodied hands are compositing using a simple matte line with a few keyframes. The orange juice is composite from two sequence, one with a full glass and one with an empty glass. The sequence of mattes is obtained by interpolating a few simple curved mattes. In the case of the clone video, the algorithm obtains a matte for each frame by finding a vertical dividing line midway between the two components of the difference video obtained when comparing the primary video and aligned secondary video (for most of the video, the midpoint of the frame can be used as the transition line).

8.3 Automatic Wire Removal

One particular kind of compositing that occurs frequently in special effects work is wire removal. After filming an empty background sequence, we can automatically remove wires using a mask attained via background subtraction. Through image filtering, our algorithm detects which parts of the mask occur in thin lines and copies background pixels at these locations (Figure 6). Cranes, platforms, and other rigging can be removed in a similar fashion, though approximate mattes may need to be manually specified for more complex objects.

In our demo video, we remove a black string that is holding up a mug. We begin by taking the difference between the primary video and aligned secondary video. The algorithm blurs this difference image in various ways and compare the values to determine which pixels belong to thin objects (the string) and not thick objects (the mug). The process is further aided with color cues (include black, exclude blue) to automatically obtain a wire matte for each frame. Once we have the matte, we use it to copy pixels from the background onto the wire. Unfortunately, due to an accidental lighting change between the primary and secondary videos, the background pixels do not perfectly match, leaving visible artifacts at the location of the wire. This problem could be eliminated using Poisson blending [27].

8.4 Replacement of Stand-Ins

A couple recent films have used actors to stand in for CG characters in order to provide a reference for other actors and/or computer animators. These stand-in actors must be replaced with the scene background when the CG character is composited into the shot (unless the CG character happens to overlap the stand-in in every pixel of every frame). Video matching can replace some of the extensive manual labor that has been used to paint a background over stand-ins for CG characters.

8.5 Wide Field-of-View Video

By matching an overlapping part of two video sequences, our method can merge them into one video sequence with a larger field of view. This differs from prior mosaicing methods [5] insofar as we produce a separate mosaic for each frame. Multiple secondary videos can expand the per-frame mosaics, so long as each sequence overlaps with another. One limitation of this approach is that moving objects cannot move from one sequence to another, unless the sequences are recorded at the same time (by placing multiple cameras on a rig).

8.6 High Dynamic Range Video

Attaining proper exposure is one of the most common and difficult problems in filmmaking. A particularly useful kind of compositing is the creation of high dynamic range video from several low dynamic range videos recorded at different exposures (Figure 7) [28]. To perform video matching across different exposures, we first normalize the local contrast and brightness (Section 4.2). In this case, we set $\sigma_{pixel} = 5$ and $\sigma_{motion} = 5$. Once the sequences have been aligned, standard techniques can be used to combine the images and remap the result for display [28, 14]. This approach can be performed on scenes that involve a moving subject, which must be properly exposed in one sequence while other sequences (without the moving subject) properly expose various parts of the background.

In our demo video, we create a high dynamic range composite using standard methods. The algorithm fits a curve to the intensity differences between the images, allowing the intensities to be mapped into a common range. Once they are in this common range, we could remap the images for display [28, 29, 14]. Instead, for simplicity, we visualize the results by selecting a range of intensities that varies smoothly from frame to frame (creating the appearance of a variable exposure).

9 Limitations and Future Work

The main limitation of our approach is that the primary and secondary video sequences must have spatially similar motions. Our method allows general camera motion (handheld, tripod-mounted, vehicle-mounted, etc.), but requires that each video sequence follow nearly the same trajectory through space (though perhaps with substantially different timing). This limitation arises partially because our algorithm does not model discontinuities in the correspondence field. We do represent variation in pixel motion due to depth, but we assume that this variation occurs smoothly across the image. Another limitation is the algorithm's dependence on 2D image texture for matching.

Both discontinuities and a lack of 2D texture are issues that are handled by many existing optical flow algorithms. However, these algorithms cannot cope with large-scale differences between the images (such as an object that appears in one image but not the other). When large image regions are unmatchable, we have barely enough information to find a smooth warping between the images; finding correct discontinuities can be difficult if not impossible.

Nonetheless, in the future we plan to extend our algorithm to make better use of the information in the images. We intend to decompose the optical motion into depth parameters and camera motion parameters. To do this, the algorithm described in this paper will be used to find correspondences for the estimation of epipolar geometry. The epipolar constraints can then be used to incorporate information from 1D edge features (not just 2D features), resulting in a better correspondence field.

We also plan to combine both inter-sequence and intra-sequence matching to improve temporal coherence and frame search efficiency. Based on the inter-sequence correspondences for one frame pair, we will select parts of each frame in which to compute intra-sequence correspondences. These intra-sequence correspondences will then be used to select a secondary frame that will match the subsequent primary frame.

10 Conclusion

This paper presents a new method for registering multiple video sequences by selecting video frames and applying image warps. We provide a method for robust image alignment that combines elements of feature-point correspondence matching and local motion estimation (i.e. optical flow). Unlike existing methods, the algorithm is explicitly designed to handle large-scale differences between images. Our method makes effective use of the information available in the image without being distracted by parts of the image that are not matchable.

We use this image registration method as a sub-routine in a video alignment algorithm that searches for a good match for each video frame. This algorithm provides a partial solution to the problem of aligning video sequences that were recorded with general camera motions. This is a valuable problem to solve and one that has attracted relatively little attention in the past.

As discussed in Section 9, the main limitations of this method are that the videos must follow spatially similar camera trajectories and that the videos must contain sufficient texture. Both of these limitations can be partially overcome by incorporating 1D image constraints.

Despite these limitations, the algorithm is useful for a variety of applications, such as foreground segmentation, compositing, wire removal, replacing stand-ins, per-frame mosaicing, and high dynamic range imaging. In the past, many of these applications required registered images from a static or robotically controlled camera. These techniques can now be applied in a wider range of situations using the methods presented in this paper.

References

[1] S. S. Beauchemin and J. L. Barron, "The computation of optical flow," *ACM Computing Surveys*, vol. 27, no. 3, pp. 433–467, 1995.

[2] Daniel Scharstein and Richard Szeliski, "A taxonomy and evaluation of dense two-frame stereo correspondence algorithms," *Int. J. Comput. Vision*, vol. 47, no. 1-3, pp. 7–42, 2002.

[3] Michael J. Black and P. Anandan, "The robust estimation of multiple motions: parametric and piecewise-smooth flow fields," *Computer Vision and Image Understanding*, vol. 63, no. 1, pp. 75–104, 1996.

[4] C.J. Harris and M. Stephens, "A combined corner and edge detector," in *4th Alvey Vision Conference*, 1988, pp. 147–151.

[5] Matthew Brown and David G. Lowe, "Recognising panoramas," in *ICCV*, 2003, pp. 1218–1225.

[6] M. A. Fischler and R. C. Bolles, "Random sample consensus: a paradigm for model fitting with applications to image analysis and automated cartography," *Communications of the ACM*, vol. 24, no. 6, pp. 381–395, 1981.

[7] R. Hartley and A. Zisserman, *Multiple View Geometry in Computer Vision*, Cambridge University Press, Cambridge, UK, 2000.

[8] Y. Kanazawa and K. Kanatani, "Robust image matching under a large disparity," in *Workshop on Science of Computer Vision*, 2002, pp. 46–52.

[9] P. Smith, D. Sinclair, R. Cipolla, and K. Wood, "Effective corner matching," in *British Machine Vision Conference*, 1998, pp. 545–556.

[10] Yaron Caspi and Michal Irani, "A step towards sequence to sequence alignment," in *CVPR*, 2000, pp. 682–689.

[11] Harpreet S. Sawhney, Yanlin Guo, Keith Hanna, Rakesh Kumar, Sean Adkins, and Samuel Zhou, "Hybrid stereo camera: an IBR approach for synthesis of very high resolution stereoscopic image sequences," in *SIGGRAPH*, 2001, pp. 451–460.

[12] Cen Rao, Alexei Gritai, and Mubarak Shah, "View-invariant alignment and matching of video sequences," in *ICCV*, 2003, pp. 939–945.

[13] Yung-Yu Chuang, Aseem Agarwala, Brian Curless, David H. Salesin, and Richard Szeliski, "Video matting of complex scenes," *ACM Trans. Graph.*, vol. 21, no. 3, pp. 243–248, 2002.

[14] Sing Bing Kang, Matthew Uyttendaele, Simon Winder, and Richard Szeliski, "High dynamic range video," *ACM Trans. Graph.*, vol. 22, no. 3, pp. 319–325, 2003.

[15] Stan Birchfield and Carlo Tomasi, "A pixel dissimilarity measure that is insensitive to image sampling," *IEEE Trans. on Pattern Analysis and Machine Intelligence*, vol. 20, no. 4, pp. 401–406, 1998.

[16] K. N. Kutulakos, "Approximate N-view stereo," in *ECCV*, 2000, pp. 67–83.

[17] Richard Szeliski and Daniel Scharstein, "Symmetric sub-pixel stereo matching," in *ECCV*, 2002, pp. 525–540.

[18] Vittorio Ferrari, Tinne Tuytelaars, and Luc Van Gool, "Real-time affine region tracking and coplanar grouping," in *CVPR*, 2001, pp. 226–233.

[19] Christopher G. Atkeson, Andrew W. Moore, and Stefan Schaal, "Locally weighted learning," *Artificial Intelligence Review*, vol. 11, no. 1-5, pp. 11–73, 1997.

[20] Alison Noble, *Descriptions of Image Surfaces*, Ph.D. thesis, Oxford University, Oxford, UK, 1989.

[21] B.D. Lucas and T. Kanade, "An iterative image registration technique with an application to stereo vision," in *Int. Joint Conf. Artificial Intelligence*, 1981, pp. 674–679.

[22] Jianbo Shi and Carlo Tomasi, "Good features to track," in *CVPR*, 1994, pp. 593–600.

[23] A. P. Dempster, N. M. Laird, and D. B. Rubin, "Maximum likelihood from incomplete data via the EM algorithm," *Journal of the Royal Statistical Society Series B*, vol. 39, no. 1, pp. 1–38, 1977.

[24] Arno Schödl, Richard Szeliski, David H. Salesin, and Irfan Essa, "Video textures," in *SIGGRAPH*, 2000, pp. 489–498.

[25] Aseem Agarwala, Mira Dontcheva, Maneesh Agrawala, Steven Drucker, Alex Colburn, Brian Curless, David Salesin, and Michael Cohen, "Interactive digital photomontage," *ACM Trans. Graph.*, p. In press, 2004.

[26] A. J. Davison, J. Deutscher, and I. D. Reid, "Markerless motion capture of complex full-body movement for character animation," in *Eurographics Workshop on Animation and Simulation*, 2001, pp. 3–14.

[27] Patrick Pérez, Michel Gangnet, and Andrew Blake, "Poisson image editing," *ACM Trans. Graph.*, vol. 22, no. 3, pp. 313–318, 2003.

[28] Paul E. Debevec and Jitendra Malik, "Recovering high dynamic range radiance maps from photographs," in *SIGGRAPH*, 1997, pp. 369–378.

[29] Frédo Durand and Julie Dorsey, "Fast bilateral filtering for the display of high-dynamic-range images," *ACM Trans. Graph.*, vol. 21, no. 3, pp. 257–266, 2002.

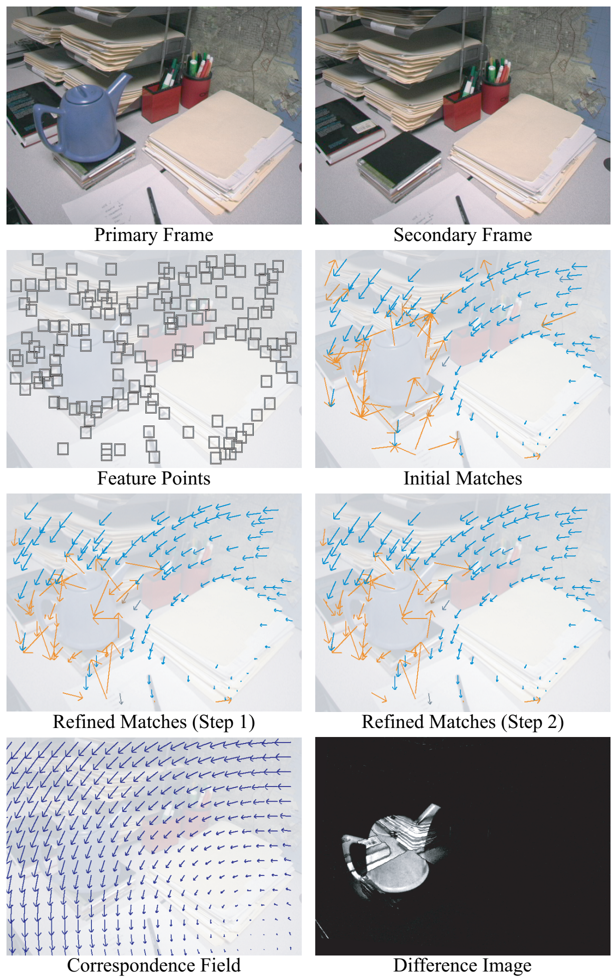

Figure 4: The image matching algorithm typically converges in a few iterations. The blue and yellow arrows denote high and low probability correspondences, respectively. The algorithm successfully recognizes that the teapot pixels cannot be matched with the background. The reconstructed dense correspondences are quite accurate, as illustrated by the difference between the primary frame and the warped secondary frame. The black regions in the difference image indicate that the background pixels are successfully matched (with a pixel difference near zero).

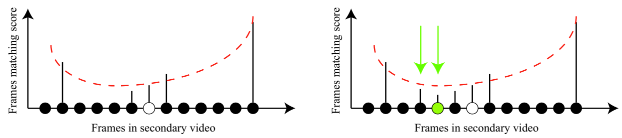

Figure 5: Given an initial guess (white circle) of which frame to use in the secondary video, we check several nearby frames (left). We fit a quadratic regression model to the frame matching scores (red dashed curve), then check frames near the minimum of the curve (green arrows). Next we refit the quadratic model and repeat the process until all near-minimal frames have been checked. Finally, we pick the frame with the lowest score (green circle).

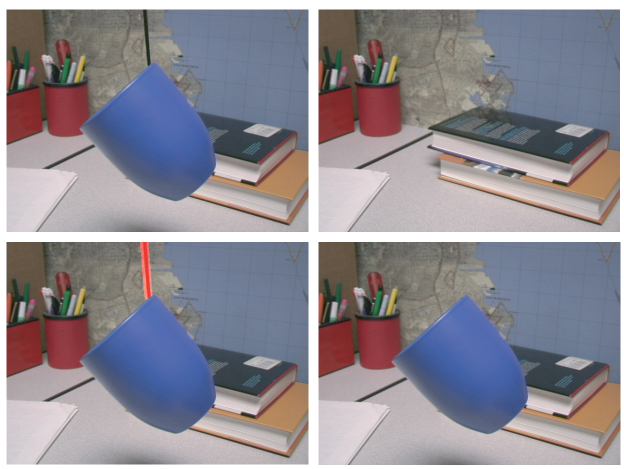

Figure 6: The top images have been registered using the robust matching algorithm. From these images we can use simple image processing methods (background subtraction and color thresholds) to create a mask for the wire (in red). Inside the mask, we copy pixels from the background. This allows a wire to be automatically removed in each frame of a long sequence from a moving camera.

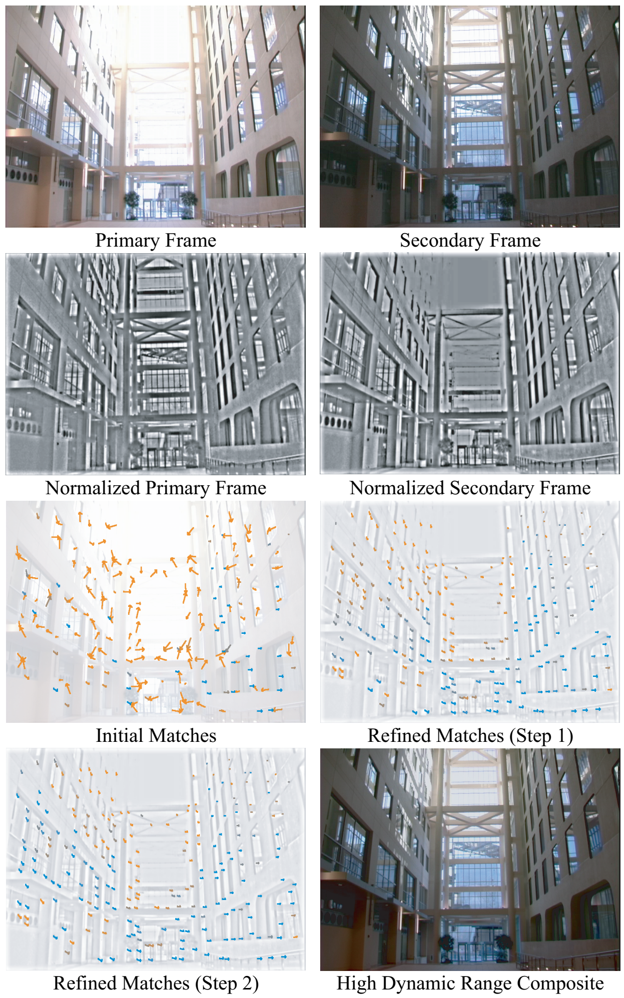

Figure 7: These frames were selected by the video matching algorithm from a pair of videos recorded at different exposures. The algorithm first performs local brightness/contrast normalization, then finds high-likelihood correspondences. Once the secondary frame has been mapped to the first, the exposures are combined to create a high dynamic range composite.

(a)
(b)
(c)
(d)
(e)
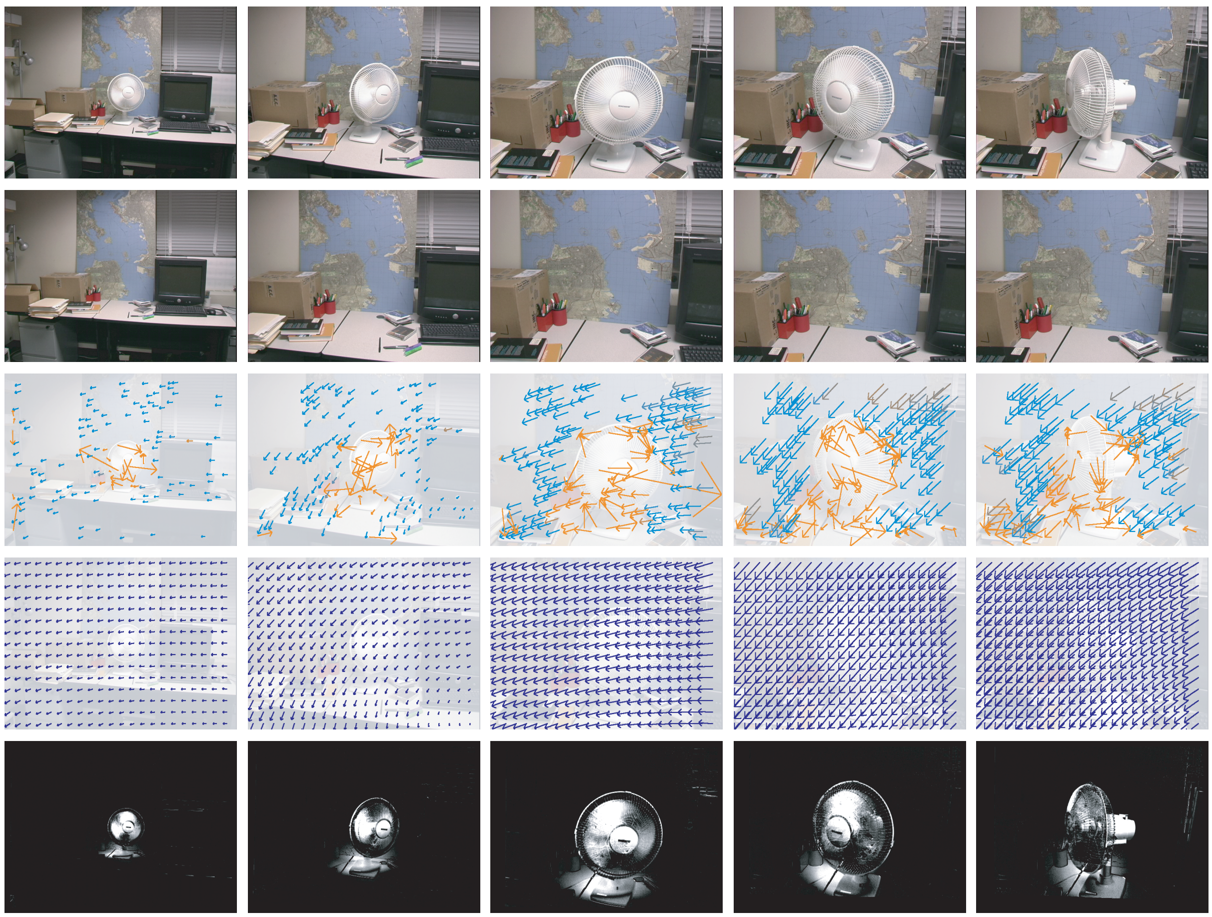

Figure 8: **(a)** Primary video frames from a hand-held sequence (frames 0, 60, 120, 180, 240). **(b)** Matching secondary video frames found by our algorithm (frames 14, 89, 138, 147, 147). **(c)** Refined correspondences found by the algorithm. **(d)** Reconstructed correspondence fields. **(e)** Difference between primary frame and projected secondary frame.

Figure 9: This figure shows primary frames **(a)**, secondary frames **(b)**, and various composites **(c)**. From left to right: **(1)** a transparent fan created by blending the two frames, **(2)** color manipulated according to a difference matte, **(3)** cloning a person by compositing the left half of one image with right half of another, **(4)** changing the amount of orange juice using a horizontal compositing line, and **(5)** a dismembered hand with a key-framed compositing line. None of the composites require per-frame manual rotoscoping.